Imaging the (un)imaginable of the Barrier Immune system

Guo, N.

Chapter 6

Summarizing discussion

In recent years, single-cell mass cytometry (CyTOF) has been used to simultaneously examine the expression of surface and intracellular proteins on single cell suspensions isolated from blood and tissue samples, to reveal disease-associated immune characteristics and identify functional biomarkers and therapeutic targets of disease[1, 2, 3, 4]. In addition, imaging mass cytometry (IMC) has been developed to enable multiplexed detection of proteins to delineate spatial cellular interactions and immune system heterogeneity in the tissue context[5, 6]. In this thesis, we have introduced the adoption of IMC on snap-frozen tissues. For this we developed a dedicated antibody panel, optimized the staining procedure, validated staining quality, and performed basic analysis of datasets by MCD™ Viewer, followed by downstream analysis based on pixels. IMC with a 36-marker panel was applied on human fetal intestine to investigate immune system development during the second trimester. Moreover, to investigate disease-associated immune subsets, IMC with a dedicated antibody panel was performed on skin biopsies from patients suffering from mycosis fungoides or psoriasis. Here, we aimed to determine whether there is a correlation between clinical parameters and IMC findings.

Imaging mass cytometry and data analysis

To enable IMC on snap-frozen tissues, we optimized the staining protocol for a 34-marker panel to obtain a high signal/noise ratio while preserving the morphology of the tissue samples. For this, we used immunohistochemistry for the primary selection of suitable antibodies. In addition, we determined the optimal drying time of the freshly cut tissue sections, compared fixation procedures, and investigated the optimal incubation condition for each of the antibodies in the panel (**Chapter 2**). Guided by the DNA (Intercalator-Ir) signal and the signal/noise ratio of each marker in MCD™ Viewer software, we determined on the optimal staining methods for the full IMC antibody panel for analysis of snap-frozen human fetal intestinal samples. In addition, this protocol was adapted for optimal performance when applied to skin tissue samples.

Multiplexed imaging data can be analyzed by visualization of the individual markers and overlays of several markers with different colors to reveal the tissue architecture and the spatial distribution and interactions between different cell types (**Chapter 2-5**). Moreover, several computational approaches have been developed to analyze all markers in the panel simultaneously, such as HistoCAT[7] and ImaCytE[8]. To extract single-cell data from the images, single cells are generated by using cell segmentation masks Ilastik and CellProfiler. To normalize variations in signal intensity and background between samples, a normalization strategy

for the processing of IMC data is applied prior to analysis by high-dimensional reduction tools[9]. Once imaging data have been segmented, downstream analysis by several approaches/algorithms can be used to identify immune and non-immune cells, the abundance of cell subsets, and the cellular neighborhoods in which these cells are present in health and disease[10, 11, 12].

We also have applied the optimized segmentation workflow to process the IMC datasets on skin biopsies of patients with psoriasis in **Chapter 5**. By comparing the DNA staining with the cell segmentation we observed that this approach is unable to accurately segment regions with a high cellular density, impacting on the cell phenotype identification and cell-cell interaction analysis (**Figure 1**). However, as such areas with dense immune infiltrates are likely to reflect disease-related cellular interactions it is important to gain more information on the composition of these immune infiltrates. For this we developed *Cytosplore imaging* to analyze the IMC data at the pixel level, by which we were able to identify and quantify individual cell types within these aggregates (**Chapter 2 and 5**). Moreover, pixel analysis enables the identification of so-called double-feature pixels, pixels containing markers of two cell types, like T cells and APCs, and thus most likely reflecting co-localization of T cells and APCs (**Chapter 5**), both potential diagnostic/therapeutic targets in both intestinal and skin diseases. Moreover, this feature of the pixel-based analysis provides semi-quantitative data on cell-cell interactions, which can be further explored by texture-aware dimensionality reduction methods to analyze spatial pixel neighborhoods by distance measures in future work[13].

The human fetal intestine

To study the development of the human fetal intestine, we applied spectral flow cytometry together with IMC to human fetal intestinal samples from week 14 through week 22 of gestation. With spectral flow cytometry, we identified distinct populations of Ki-67 expressing cells within all major immune subsets present in the samples. Moreover, the percentage of Ki-67$^+$ cells in these immune subsets remained constant throughout the second trimester of gestation, suggesting that there is a continuous pool of proliferating cells to populate the growing fetal intestine. Since the majority of the immune cells in the fetal intestine expressed CD127 (IL-7 receptor, IL-7R), IL-7 was used to stimulate the fetal immune cells to investigate the proliferative potential *in vitro*. Here we observed proliferation of fetal immune cells that was enhanced by the presence of IL-7 and accompanied by upregulation of CD40L and granzyme B expression, providing evidence that the observed Ki-67 expression reflected proliferative potential of fetal intestinal

immune cells. In addition, we performed RNAscope analysis which allows the visualization of selected RNA molecules with high sensitivity *in situ*[14]. Here, we observed the presence of IL-7 transcripts in both the lamina propria and epithelium of a human fetal intestinal sample from gestational week 14 (**Figure 2A-C**), suggesting that fetal intestinal cells can produce IL-7 during fetal development supporting immune cell proliferation. Future elucidation of the cell types producing IL-7 in the human fetal intestine would require a combination of RNAscope and IMC. This combination of techniques has been successfully applied to chemokine expression analysis in tumor samples[15] and should be feasible to be used for analysis of the human fetal intestine as well. This will be the subject of further studies.

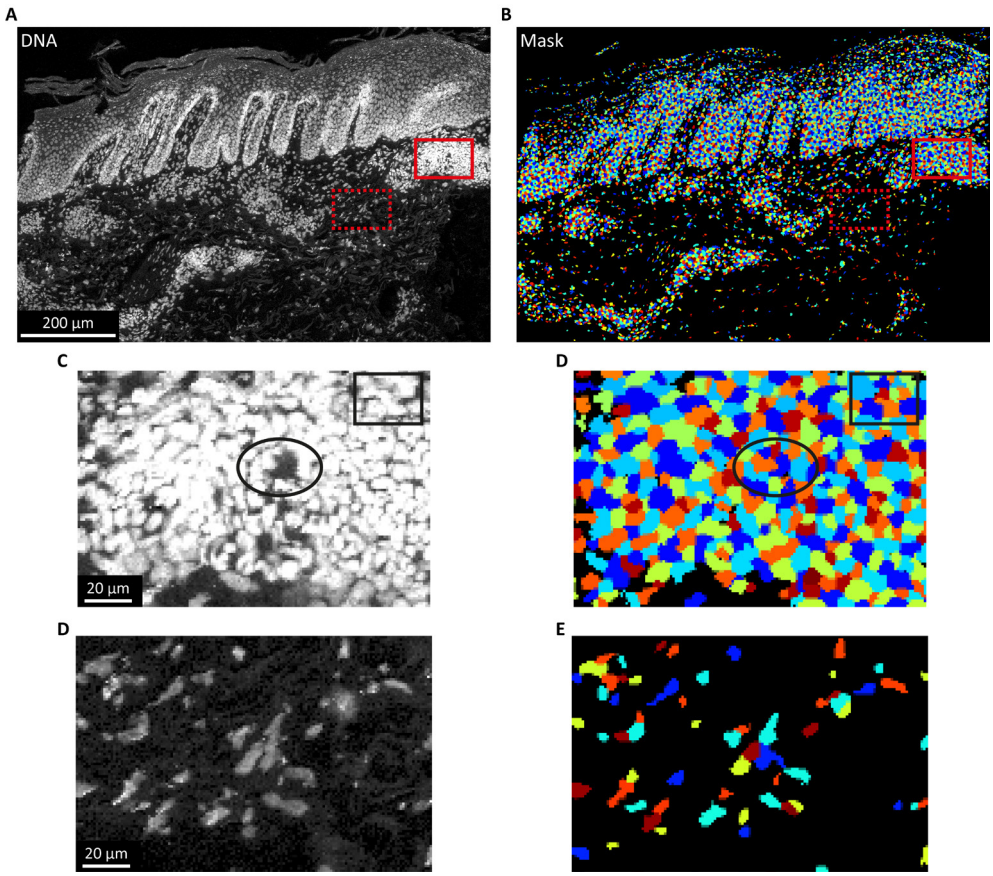

Figure 1 Generation of single cell masks in a representative ROI from a psoriatic lesion. (A) DNA staining performance colored by white in MCD™ viewer. A region with high-density cells is boxed by the solid line, while a region with low-density cells boxed by a dashed line. **(B)** Single cell masks by Ilastic and CellProfiler. Colors are used for visualization of individual cells. **(C-D)** DNA staining and cell mask for the region with high cellular density. **(E-F)** DNA staining and cell mask for the region with low cellular density.

IMC identified formation of lymphoid follicles (LFs) in the developing intestine just below the epithelium from week 16 onwards, harboring B cells, T cells, ILCs and myeloid cells. Also, Ki-67 positive cells were detected in all major immune subsets both in the LF and in the lamina propria. As described previously, the chemokine CXCL13 has an important role in the formation of secondary lymphoid organs by mediating the influx of mature lymphocytes into the newly forming follicles and regulating the recruitment of LTi cells[16]. CXCL13 expression has also been detected in lymphoid follicles present in inflamed tissue sites, for example ulcerative colitis[17]. RNAscope analysis of the human fetal intestine revealed the presence of CXCL13 in the lamina propria of a human fetal intestinal sample from gestational week 14 (**Figure 2D**), where the location and distribution of the CXCL13 signal fits with the location and distribution of lymphoid follicles identified by IMC. Further investigations are needed to explore the role of CXCL13 in the formation of lymphoid follicles in the developing fetal intestine.

Moreover, our IMC data revealed abundant expression of CD161 and CD69 in the LF of human fetal intestines (**Chapter 3**). In addition, further analysis by spectral flow cytometry showed that $CD161^{+}CD69^{+}$ T and $CD3^{-}CD7^{+}$ ILCs cells co-expressed CD117, CD127 and CCR6 (**Chapter 3**). These data fit with the observation that in the murine small and large intestinal mucosa a large fraction of closely packed lymphocytes in cryptopatches expressed CD117 and CD127, pointing to the presence of T and/or B lympho-hemopoietic progenitors[18]. Moreover, our data indicate that a subset of $CD161^{+}CD69^{+}CD117^{+}CD127^{+}CCR6^{+}$ cells expressed Ki-67, compatible with cellular proliferation. Additional work is needed to determine whether these Ki-67^{+} cells represent a stable subset or a transitional phenotype in the human fetal intestine.

Formation of $CD4^{+}$ T cell memory in the human fetal intestine

Previously, we revealed the presence of memory $CD4^{+}$ and $CD8^{+}$ T cells in human fetal intestine[19], suggesting *in utero* exposure to foreign antigens. Additional observations showed that memory formation was associated with several signaling pathways, including that of the T cell receptor. However, whether fetal T cells are exposed to foreign antigens is still a matter of debate. In this thesis we have expanded on our initial observations by studying the proliferative capacities of the fetal intestinal immune compartment across the second gestational trimester. We have also described for the first time the formation of organized lymphoid structures in the fetal intestine (**Chapter 3**).

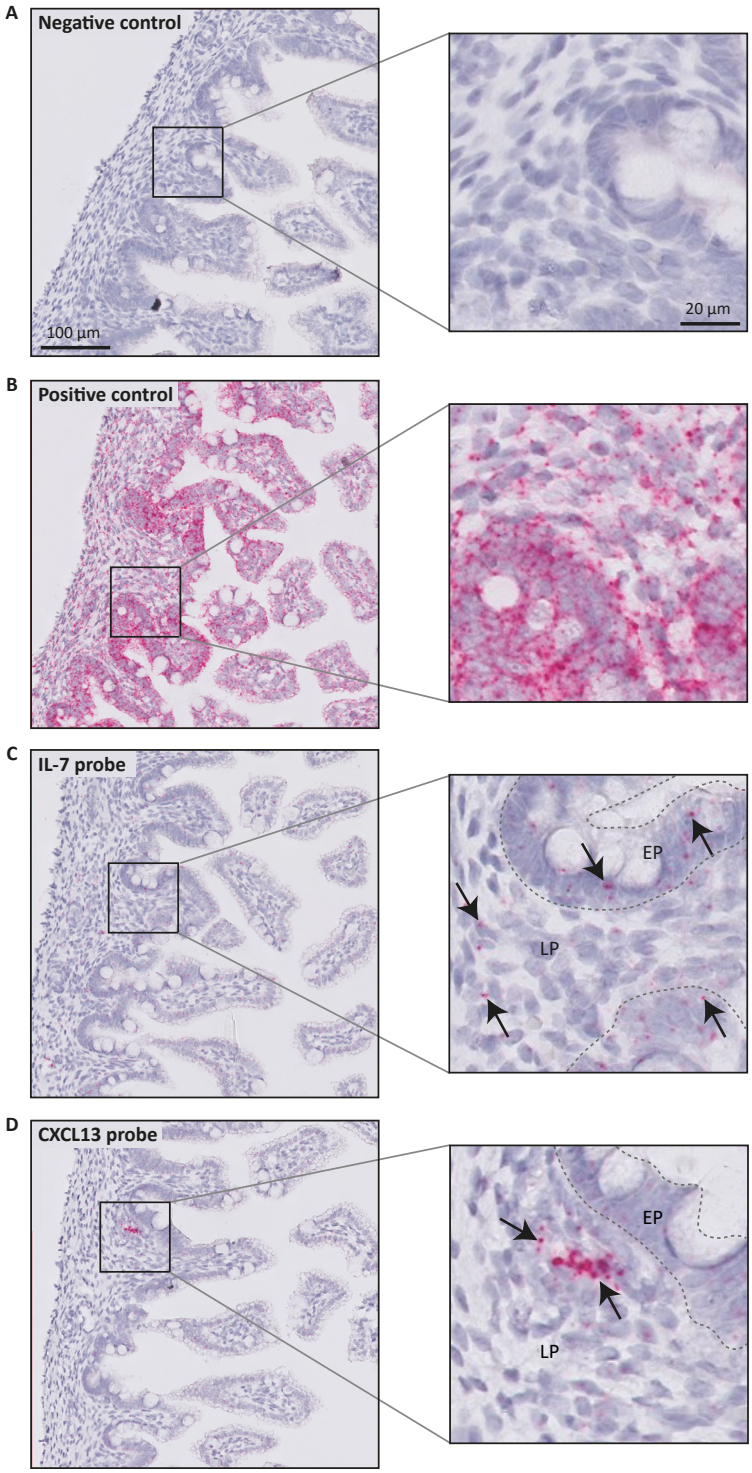

Figure 3 RNAscope detection of RNA in a FFPE human fetal intestinal sample from gastational week 14.
(A) Negative control *PPIB* probe.
(B) Positive control *DapB* probe.
(C) IL-7 probe.
(D)CXCL13 probe.
Nuclei were counterstained with hematoxylin.
EP, epithelium;
LP, lamina propria.

With these new data in mind, we can envision two scenarios for the *in utero* formation of CD4⁺ T cell memory (**Figure 3**):

1) Naive CD4⁺ T cells migrate from the thymus to mucosal inductive sites (Mesenteric lymph nodes or LFs in the lamina propria), where they encounter antigen-presenting DCs and differentiate into mucosal-imprinted memory T cells, as has been described for adult intestinal mucosa[20, 21, 22]. Then they migrate to effector sites in the fetal intestine.
2) Naive CD4⁺ T cells migrate directly from the thymus to the fetal intestinal lamina propria, where they encounter abundant proliferation signals that lead to their expansion and acquisition of a memory-like phenotype, as has been described for lymphopenia-induced proliferation[23, 24, 25].

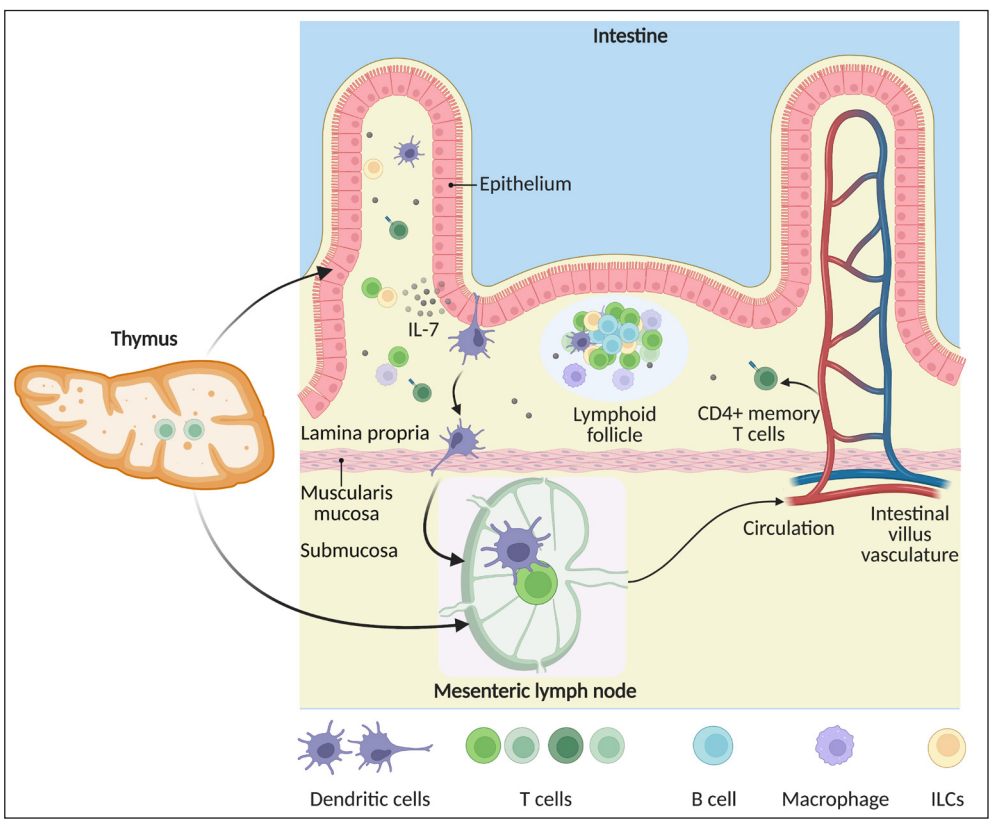

Figure 3. Depiction of memory formation in human fetal intestines. Created in Biorender.com.

Scenario 1: Memory formation at induction sites

For the first scenario to be plausible, two conditions have to be met. First, mature

inductive sites where DCs and naïve T cells can meet have to be present. Second, foreign antigen has to be available for the DCs to present.
Mesenteric lymph nodes (MLNs) are key sites for the generation of memory T cells with mucosal imprinting[26, 27]. What do we know about the timeline of human MLN development? In the human fetus, T lymphocyte differentiation is initiated in the thymus at 7-9 post-gestational weeks (PGW), and the first TCRab T cells leave the thymus by 12PGW[28]. The first lymphoid cells can be found in the lymph node (LN) primordium at 12 PGW, while monocytes and macrophages can be found from 13 PGW onwards[29]. In the 14 PGW, lymphoid cells with features of immature precursor-type thymocytes gradually fill in the cortex of the LNs[30], indicating that these cells migrate directly from the thymus to LNs. In the human fetus, MLNs can be detected as early as 13 PGW[31]. Although not determined yet for MLNs, in axillary LNs at 14 PGW, $CD4^+$ T cells are distributed throughout the anlage[32]. Meanwhile, B cells are found mainly in the outer cortex, although not yet organized in follicles, and during subsequent weeks, loosely aggregated primary follicles emerge[32, 33]. This timeline coincides with the gradual filling of LFs in the fetal intestine described in **Chapter 3**, and suggests that mucosal inductive sites develop throughout the entire second gestational trimester, and points to a plausible interaction between T cells and DCs. In support of this, in **Chapter 2**, T cells were detected in close proximity to $CD11c^+$ myeloid cells and $CD163^+$ macrophages in the lamina propria of human fetal intestines, supporting antigen uptake and presentation by myeloid cells. In **Chapter 3**, we identified proliferating naïve and memory T cells, as well as $CD1c^+$ B cells and lymphoid tissue inducer cells by suspension flow cytometry from 14 PGW onwards. Moreover, IMC analysis of human fetal intestines showed the presence of locally proliferating cells within lymphoid follicles and lamina propria as early as 16 PGW. Although the nature of the antigen is yet to be determined, the spatial distribution of T cells and APCs in the LFs supports the hypothesis of LFs as mucosal inductive sites.

Scenario 2: Lymphopenia-like expansion of naïve T cells, with acquisition of a memory-like phenotype

T cell survival and proliferation depend on availability of cytokines provided by other cell types (e.g. epithelial cells, stromal cells). Gamma-chain cytokines (including IL-2, IL-4, IL-7, IL-9 and IL-15), which share the common gamma chain cytokine receptor subunit, play an essential role in maintaining T cell memory[34], especially IL-7[35]. In LNs, the expression of IL-7 together with the CCR7 ligands (CCL19 and CCL21) by fibroblastic reticular cells attracts $CCR7^+$ T cells and provides signals for their survival[36]. Our data reveals that IL-7 can induce proliferation of naïve and memory T cells of human fetal intestine in vitro. Moreover, IL-7 transcript can

be found in both the epithelium and lamina propria in the human fetal intestine (Figure 3C). Thus, the formation of T cells with a memory phenotype in the fetal intestine can also be due to cytokine-driven expansion to populate the growing organ.

In summary, at the moment we could find evidence supporting both scenarios. Future studies are needed to further elucidate the contribution of APCs in LFs and IL-7 to the generation of memory-like $CD4^+$ T cells in the human fetal intestine.

Possible improvements of diagnostic process for Mycosis Fungoides

Currently, the diagnosis of mycosis fungoides (MF) is based on immunopathological criteria, that helps with determining the atypical lymphocytes suggestive for "cancer cells". Besides an atypical form, atypical lymphocytes show loss of immunophenotypic markers like CD2, CD3, CD5 and/or CD7 (**Table 1**)[37]. Nevertheless, some reactive dermatitis may have an atypical reactive infiltrate with marker loss like CD7, making it difficult to diagnose MF at an early stage. In those cases T-cell clonality might help, but is not entirely conclusive. For improvement of the current diagnostic process, it may be helpful if we understand the tumor microenvironment in more detail, to help in differentiating a tumor microenvironment from a reactive microenvironment. New techniques including single-cell suspension mass cytometry (CyTOF) and imaging mass cytometry (IMC) can facilitate the understanding of this microenvironment in more detail.

Table 1 Immunopathologic algorithm for diagnosis of early MF. (Table adapted from Pimpinelli et al. 2005)

Immunopathologic Criteria	**Scoring system**
1) < 50% $CD2^+$, $CD3^+$, and/or $CD5^+$ T cells	1 point for one or more criteria
2) < 10% $CD7^+$ T cells	
3) Epidermal/dermal discordance of CD2, CD3, CD5, or CD7	

In **Chapter 4**, we used CyTOF and IMC to profile the tissue resident immune cells of 10 patients with early stage of mycosis fungoides. Based on single-cell suspension data in **Chapter 4**, the shared clusters of $CD5^+CD127^+$ effector memory T cells and $CD5^+CD127^-CD25^+$ Treg-like cells were identified among these early stage MF patients. Furthermore, $CD11c^+CD14^+$ myeloid cells and $HLA\text{-}DR^+CD1a^+$ DCs were observed in the majority of MF patients. In addition, IMC revealed the co-localization of T cells with phenotypically distinct subsets of dendritic cells

(DCs) in immune aggregates in the dermis of MF patients. Altogether, these new insights might provide a basis for further studies aiming to distinguish the MF microenvironment from that in reactive dermatitis. Furthermore, a study with larger sample sizes and healthy controls will be needed to elucidate the possible prognostic value of interfering T-DCs interactions in MF.

In addition, several reports have shown that up to 15% of early-stage patients experience disease progression to advanced stage MF with an estimated 5-year survival of 24%[38, 39]. In early stage of MF, CXCR3 as interferon (IFN)-inducible chemokine receptor, induced by the IFN-γ, was up-regulated in malignant lymphocytes[40, 41]. In the advanced stage of MF, however, malignant T cells expressed more CCR4 than CXCR3[42]. As CCR4 has been described as the receptor for CCL22, primarily produced by DCs in dermis, it is likely that the interaction between CCR4 and CCL22 is involved in DCs-T stimulation[43]. Recently, scRNAseq analysis for skin tumor cells from patient with advanced stage MF revealed that malignant tumor infiltrating T lymphocytes highly expressed genes related to cell cycle progression and proliferation, and checkpoint molecules including TIM3, PD1, LAG3 and CTLA-4[44]. Moreover, gene expression profiling corroborated positive correlations between increased expression of checkpoint inhibitors and higher tumor stage of disease[45]. So it might be very useful to use CyTOF and IMC to evaluate the expression patters of these chemokine receptors and ligands, and markers indicative of cell regulation and proliferation in future experiments as well to gain better insight into the factors that play a role in the progression of early stage MF to advanced stage MF, results that may be useful for the development of better prognostics and targeted therapeutics in the future.

Future perspectives of psoriasis

Psoriasis is a chronic inflammatory skin disorder characterized by keratinocyte hyperproliferation and differentiation combined with immune cell infiltration. It is known that in the psoriatic dermis mature myeloid dendritic cells (DCs) aggregate with skin infiltrating T cells[46, 47]. Here, IL-23/IL-20-producing DCs have the potential to activate Th17 cells in psoriasis[48], causing the proliferation seen within psoriatic lesions[49]. Moreover, pathogenic Th17 cells are sustained by IL-23 within the dermis[50, 51]. In addition, keratinocytes produce additional cytokines, such as IFN-α, IL-6, and IL-10, resulting in epidermal hyperplasia[52, 53].

In **Chapter 5**, we applied imaging mass cytometry to compare lesional skin with non-lesional skin from patients with psoriasis in a proof of principle study

to determine if it would be useful to apply this technique to gain further insight into the cellular interactions that underlie psoriasis. We observed that psoriatic lesions contained prominent immune aggregates with many T cells and DCs in the dermis. Moreover, multiple types DCs subsets were observed. For more detailed analysis of the results we made use of pixel-based which allowed the visualization of the structure of psoriatic skin and the distribution and quantification of T and myeloid cell subsets. Moreover, this approach identified clusters of pixels presenting with features of both T cells and myeloid cells, likely representing direct contact between T cells and myeloid cells. This identified patients displaying frequent interactions between T cells and $CD207^{+}CD1c^{+}$ LC-like DCs in the dermis. In addition, interactions between T cells and $CD207^{-}CD1c^{+}$ DCs and between T cells and $CD206^{+}$ macrophages were observed but these varied substantially between patients. This allowed a preliminary classification of patients based on the presence of particular cell subtypes and interactions between those cell subtypes. However, further work is required determine if this relates to disease severity. It will be particularly rewarding to investigate if such differences between patients correlate to response to treatment and as such may be useful to distinguish potential responders to treatment. Moreover, it may provide leads for the development of novel therapeutic strategies.

Concluding remarks

In conclusion, the work described in this thesis demonstrates that imaging mass cytometry can provide novel information on the nature and organization of the immune system within the tissue context at barrier sites like the human intestine and skin. Our work on the human fetal intestine shows that in combination with single cell technologies this revealed a prominent role for IL-7-driven local immune cells proliferation to allow for the formation of complex organized lymphoid follicles and to fill up the immune system in the rapidly growing organ. Our work on mycosis fungoides and psoriasis indicates that imaging mass cytometry can be used to identify both disease-specific and patient-specific patterns in the composition and local organization of the immune system. Further work is needed to determine if this will be useful for patient classification and to predict response to treatment.

Reference

1. Hartmann, F.J. *et al.* High-dimensional single-cell analysis reveals the immune signature of narcolepsy. *Journal of Experimental Medicine* **213**, 2621-2633 (2016).
2. Irish, J.M. *et al.* Single Cell Profiling of Potentiated Phospho-Protein Networks in Cancer Cells. *Cell* **118**, 217-228 (2004).
3. Bruggner, R.V., Bodenmiller, B., Dill, D.L., Tibshirani, R.J. & Nolan, G.P. Automated identification of stratifying signatures in cellular subpopulations. *Proceedings of the National Academy of Sciences* **111**, E2770-E2777 (2014).
4. de Vries, N.L. *et al.* High-dimensional cytometric analysis of colorectal cancer reveals novel mediators of antitumour immunity. *Gut* **69**, 691-703 (2020).
5. Schulz, D. *et al.* Simultaneous Multiplexed Imaging of mRNA and Proteins with Subcellular Resolution in Breast Cancer Tissue Samples by Mass Cytometry. *Cell Syst* **6**, 25-36.e25 (2018).
6. Giesen, C. *et al.* Highly multiplexed imaging of tumor tissues with subcellular resolution by mass cytometry. *Nature Methods* **11**, 417-422 (2014).
7. Schapiro, D. *et al.* histoCAT: analysis of cell phenotypes and interactions in multiplex image cytometry data. *Nature Methods* **14**, 873-876 (2017).
8. Somarakis, A., Unen, V.V., Koning, F., Lelieveldt, B. & Höllt, T. ImaCytE: Visual Exploration of Cellular Micro-Environments for Imaging Mass Cytometry Data. *IEEE Transactions on Visualization and Computer Graphics* **27**, 98-110 (2021).
9. Ijsselsteijn, M.E., Somarakis, A., Lelieveldt, B.P.F., Höllt, T. & de Miranda, N. Semi-automated background removal limits data loss and normalizes imaging mass cytometry data. *Cytometry A* **99**, 1187-1197 (2021).
10. Damond, N. *et al.* A Map of Human Type 1 Diabetes Progression by Imaging Mass Cytometry. *Cell Metab* **29**, 755-768.e755 (2019).
11. Keren, L. *et al.* A Structured Tumor-Immune Microenvironment in Triple Negative Breast Cancer Revealed by Multiplexed Ion Beam Imaging. *Cell* **174**, 1373-1387.e1319 (2018).
12. Krop, J. *et al.* Imaging mass cytometry reveals the prominent role of myeloid cells at the maternal-fetal interface. *iScience* **25**, 104648 (2022).
13. Vieth, A., Vilanova, A., Lelieveldt, B., Eisemann, E. & Höllt, T. Incorporating Texture Information into Dimensionality Reduction for High-Dimensional Images. 2022 IEEE 15th Pacific Visualization Symposium (PacificVis); 2022: IEEE; 2022. p. 11-20.
14. Wang, F. *et al.* RNAscope: a novel in situ RNA analysis platform for formalin-fixed, paraffin-embedded tissues. *J Mol Diagn* **14**, 22-29 (2012).
15. Hoch, T. *et al.* Multiplexed imaging mass cytometry of the chemokine milieus in melanoma characterizes features of the response to immunotherapy. *Sci Immunol* **7**, eabk1692 (2022).
16. Marchesi, F. *et al.* CXCL13 expression in the gut promotes accumulation of IL-22-producing lymphoid tissue-inducer cells, and formation of isolated lymphoid follicles. *Mucosal Immunol* **2**, 486-494 (2009).
17. Carlsen, H.S., Baekkevold, E.S., Johansen, F.E., Haraldsen, G. & Brandtzaeg, P. B cell attracting chemokine 1 (CXCL13) and its receptor CXCR5 are expressed in normal and aberrant gut associated lymphoid tissue. *Gut* **51**, 364-371 (2002).
18. Kanamori, Y. *et al.* Identification of novel lymphoid tissues in murine intestinal mucosa where clusters of c-kit+ IL-7R+ Thy1+ lympho-hemopoietic progenitors develop. *J Exp Med* **184**, 1449-1459 (1996).
19. Li, N. *et al.* Memory CD4(+) T cells are generated in the human fetal intestine. *Nat Immunol* **20**, 301-312 (2019).
20. Buettner, M. & Bode, U. Lymph node dissection--understanding the immunological function of lymph nodes. *Clin Exp Immunol* **169**, 205-212 (2012).
21. Houston, S.A. *et al.* The lymph nodes draining the small intestine and colon are anatomically separate and immunologically distinct. *Mucosal Immunol* **9**, 468-478 (2016).
22. Iwata, M. *et al.* Retinoic acid imprints gut-homing specificity on T cells. *Immunity* **21**, 527-538 (2004).
23. Min, B. *et al.* Neonates support lymphopenia-induced proliferation. *Immunity* **18**, 131-140 (2003).
24. Guimond, M. *et al.* Interleukin 7 signaling in dendritic cells regulates the homeostatic proliferation and niche size of CD4+ T cells. *Nat Immunol* **10**, 149-157 (2009).
25. Surh, C.D. & Sprent, J. Homeostasis of naive and memory T cells. *Immunity* **29**, 848-862 (2008).
26. Huang, F.P. *et al.* A discrete subpopulation of dendritic cells transports apoptotic intestinal epithelial cells to T cell areas of mesenteric lymph nodes. *J Exp Med* **191**, 435-444 (2000).
27. Sheridan, B.S. & Lefrançois, L. Regional and mucosal memory T cells. *Nat Immunol* **12**, 485-491 (2011).
28. Lobach, D.F. & Haynes, B.F. Ontogeny of the human thymus during fetal development. *J Clin Immunol* **7**, 81-97 (1987).
29. Markgraf, R., von Gaudecker, B. & Müller-Hermelink, H.K. The development of the human lymph node. *Cell and Tissue Research* **225**, 387-413 (1982).
30. von Gaudecker, B. & Müller-Hermelink, H.K. The development of the human tonsilla palatina. *Cell Tissue Res* **224**, 579-600 (1982).

31. Cupedo, T., Nagasawa, M., Weijer, K., Blom, B. & Spits, H. Development and activation of regulatory T cells in the human fetus. *Eur J Immunol* **35**, 383-390 (2005).
32. Asano, S. *et al.* Immunohistologic detection of the primary follicle (PF) in human fetal and newborn lymph node anlages. *Pathol Res Pract* **189**, 921-927 (1993).
33. Westerga, J. & Timens, W. Immunohistological analysis of human fetal lymph nodes. *Scand J Immunol* **29**, 103-112 (1989).
34. Lantz, O., Grandjean, I., Matzinger, P. & Di Santo, J.P. Gamma chain required for naïve CD4+ T cell survival but not for antigen proliferation. *Nat Immunol* **1**, 54-58 (2000).
35. Tan, J.T. *et al.* IL-7 is critical for homeostatic proliferation and survival of naive T cells. *Proc Natl Acad Sci U S A* **98**, 8732-8737 (2001).
36. Link, A. *et al.* Fibroblastic reticular cells in lymph nodes regulate the homeostasis of naive T cells. *Nature Immunology* **8**, 1255-1265 (2007).
37. Pimpinelli, N. *et al.* Defining early mycosis fungoides. *J Am Acad Dermatol* **53**, 1053-1063 (2005).
38. Talpur, R. *et al.* Long-term outcomes of 1,263 patients with mycosis fungoides and Sézary syndrome from 1982 to 2009. *Clin Cancer Res* **18**, 5051-5060 (2012).
39. Scarisbrick, J.J. *et al.* Cutaneous Lymphoma International Consortium Study of Outcome in Advanced Stages of Mycosis Fungoides and Sézary Syndrome: Effect of Specific Prognostic Markers on Survival and Development of a Prognostic Model. *J Clin Oncol* **33**, 3766-3773 (2015).
40. Lu, D. *et al.* The T-cell chemokine receptor CXCR3 is expressed highly in low-grade mycosis fungoides. *Am J Clin Pathol* **115**, 413-421 (2001).
41. Kuo, P.T. *et al.* The Role of CXCR3 and Its Chemokine Ligands in Skin Disease and Cancer. *Front Med (Lausanne)* **5**, 271 (2018).
42. Sugaya, M. Chemokines and cutaneous lymphoma. *J Dermatol Sci* **59**, 81-85 (2010).
43. Wu, M., Fang, H. & Hwang, S.T. Cutting edge: CCR4 mediates antigen-primed T cell binding to activated dendritic cells. *J Immunol* **167**, 4791-4795 (2001).
44. Gaydosik, A.M. *et al.* Single-Cell Lymphocyte Heterogeneity in Advanced Cutaneous T-cell Lymphoma Skin Tumors. *Clin Cancer Res* **25**, 4443-4454 (2019).
45. Querfeld, C. *et al.* Primary T Cells from Cutaneous T-cell Lymphoma Skin Explants Display an Exhausted Immune Checkpoint Profile. *Cancer Immunol Res* **6**, 900-909 (2018).
46. Zaba, L.C. *et al.* Amelioration of epidermal hyperplasia by TNF inhibition is associated with reduced Th17 responses. *J Exp Med* **204**, 3183-3194 (2007).
47. Kim, T.-G. *et al.* Dermal Clusters of Mature Dendritic Cells and T Cells Are Associated with the CCL20/CCR6 Chemokine System in Chronic Psoriasis. *Journal of Investigative Dermatology* **134**, 1462-1465 (2014).
48. Wang, F. *et al.* Prominent production of IL-20 by CD68+/CD11c+ myeloid-derived cells in psoriasis: Gene regulation and cellular effects. *J Invest Dermatol* **126**, 1590-1599 (2006).
49. Schön, M.P. & Boehncke, W.-H. Psoriasis. *New England Journal of Medicine* **352**, 1899-1912 (2005).
50. Lee, Y. *et al.* Induction and molecular signature of pathogenic TH17 cells. *Nature Immunology* **13**, 991-999 (2012).
51. Lowes, M.A., Russell, C.B., Martin, D.A., Towne, J.E. & Krueger, J.G. The IL-23/T17 pathogenic axis in psoriasis is amplified by keratinocyte responses. *Trends in Immunology* **34**, 174-181 (2013).
52. Page, K.M. *et al.* Molecular and Cellular Responses to the TYK2/JAK1 Inhibitor PF-06700841 Reveal Reduction of Skin Inflammation in Plaque Psoriasis. *J Invest Dermatol* **140**, 1546-1555. e1544 (2020).
53. Sohn, S.J. *et al.* A restricted role for TYK2 catalytic activity in human cytokine responses revealed by novel TYK2-selective inhibitors. *J Immunol* **191**, 2205-2216 (2013).